RELATION BETWEEN ENSO AND TROPICAL CYCLONES IN THE WNP SIMULATED IN A CGCM

P5.3

Satoshi Iizuka, Tomonori Matsuura, Mitsutaka Fujita, and Hironori Fudeyasu

National Research Institute for Earth Science and Disaster Prevention

1. Introduction

The interannual variation in tropical cyclone activities over the western North Pacific (WNP) has been investigated by several studies (Lander 1993, 1994; Chan et al., 1998, Chan 2000; Chia and Ropelewski, 2002; Wang and Chan, 2002), focusing on the relation with El Niño / Southern Oscillation (ENSO), although the variations with quasi-biennial (Chan, 1995) and inter-decadal time scales (Yumoto and Matsuura, 2001; Matsuura et al., 2003) are also found. These studies show that ENSO causes the zonal shift in the mean genesis locations of tropical cyclones: tropical cyclones tend to form more eastward (westward) during El Niño (La Niña) years than normal. Furthermore, tropical cyclones in September- November tend to recurve more northeastward during strong El Niño years, whereas most of tropical cyclones take a westward traveling course during strong La Niña years (Wang and Chan, 2002). Moreover, the number of tropical cyclones making landfall in China, the Indochina Peninsula, the Malay Peninsula, and the Philippines, is significantly less than normal in September- November of El Niño years (Elsner and Liu, 2003; Wu et al., 2004).

In the present study, we re-examine the impact of ENSO on tropical cyclone activities over the WNP, using the observations and the simulation of a high-resolution coupled ocean atmosphere general circulations model (CGCM).

2. Model and Data

The atmospheric part of the CGCM is the global spectral model which has previously used as a forecasting model at the Japan Meteorological Agency. In the horizontal direction, all variables are truncated at total wave number 213 (T213). There are 21 levels in the vertical from the surface to approximately 10 hPa. The ocean component is based on the Southampton- East Anglia model (e.g. Killworth et al., 1991). The model domain covers the global oceans except for the Arctic Ocean, where the observed climatological sea surface temperature (SST) and sea-ice distributions are prescribed as the boundary conditions of the atmospheric model. The horizontal resolution is 0.5625º, with 37 vertical levels. Other details for the CGCM are given in Iizuka et al. (2003). The CGCM was integrated for 100 years without flux correction, and we analyzed the results for 81-year periods from year 20 to year 100.

The best track data compiled by the Joint Typhoon Warning Center is used to identify the genesis locations and tracks of observed tropical cyclones. The National Center for Environmental Prediction- National Center for Atmospheric Research (NCEP- NCAR) global atmospheric reanalysis data is also used to reveal the relation between atmospheric circulations and tropical

Corresponding author address: Satoshi Iizuka, National Research Institute for Earth Science and Disaster Prevention, Tennodai 3-1, Tsukuba, Ibaraki, Japan 305-0006; e-mail: iizuka@bosai.go.jp

cyclone activity for comparing the simulation with the observations.

3. Results

3.1 Definitions of tropical cyclones

The various definitions have been proposed to detect tropical cyclones simulated in GCMs (e.g. Camargo and Zebiak, 2002). We here used the following definitions to identify tropical cyclones simulated in the CGCM.

1. The grid point with minimum sea level pressure in a 9x9 grid-point box is defined as the center of a tropical cyclone.

2. The difference in sea level pressure between the center and each grid point on the boundaries at 4 grid points away from the center is greater than 5 hPa.

3. Maximum surface wind speeds in a 9x9 grid-point box around the center are greater than 17m/s.

4. The difference in vorticity of surface winds between the center and each grid point on the boundaries at 4 grid points away from the center greater than 1.5×10^{-4} s^{-1}.

5. The lifetime is more than 2 days.

6. The genesis location is located to the south of 30ºN.

7. The detected tropical cyclone passes over the region between 100ºE and 180º.

8. Vorticity of surface winds around the center has the value greater 5.0×10^{-4} s^{-1} than at least 4 times through its lifetime.

The most above criteria are used to exclude extratropical cyclones and weak tropical storms.

3.2 Climatology of tropical cyclones

We first present the climatology of model SST and surface wind during summer (July-August) (Fig. 1). The overall feature of the simulated SST is in reasonably agreement with the observed SST, although there is the warm SST bias in the southeastern tropical Pacific as seen in other CGCMs. The warm SST region higher than 26ºC exists over the WNP. The model surface wind patterns are also similar to the observation, although the simulated cross equatorial winds in the WNP are weaker.
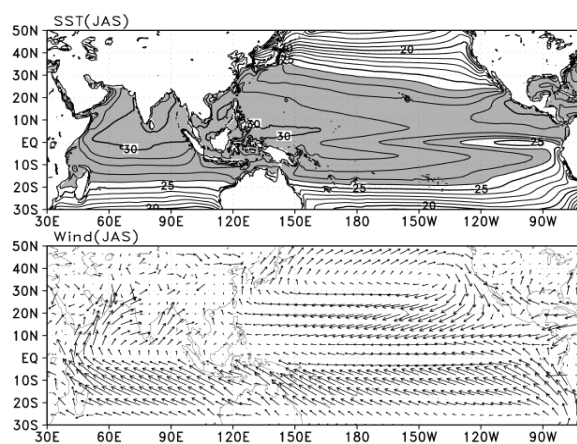

Figure 1: Climatology of model SST (upper) and surface wind (lower) during summer (July-August). Contour interval is 1ºC and shaded regions indicate SST higher than 26ºC.
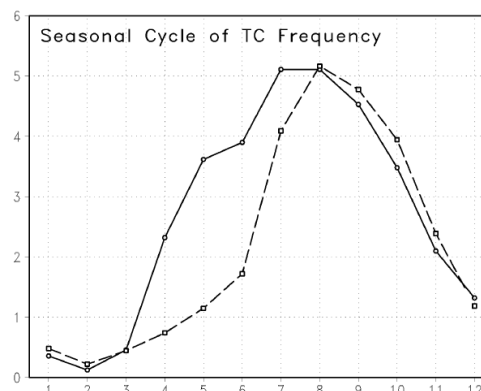

Figure 2: Seasonal frequency of the model (thick line) and observed (dashed line) tropical cyclones.
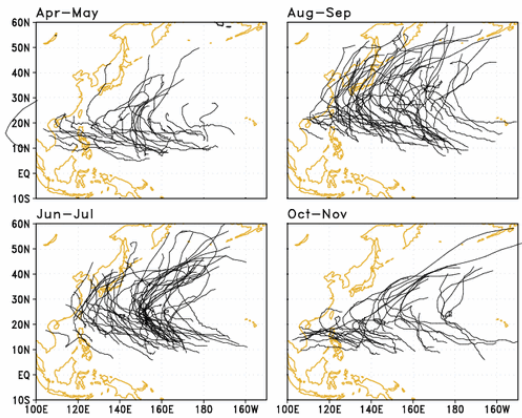
Figure 3: Tracks of the model tropical cyclones during the period from year 20 to year 24 for April-May (upper left), June-July (lower left), August-September (upper right), and October-November (lower right).
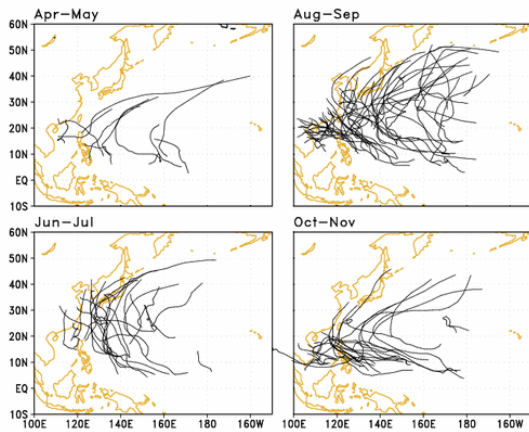

Figure 4: Same as in Fig. 3, but for the observed tropical cyclones during the period from1995 to 2000.

Figure 2 presents the climatological seasonal cycle of frequency of the simulated tropical cyclones. The annual number of the model tropical cyclone is about 32, which is greater than the observation (27) averaged during the period from 1951 to 2004. The discrepancy is related to the model bias that more tropical cyclones tend to be formed around the central tropical Pacific from April to July. The same deficiencies are found in the results of the atmospheric model of the CGCM when it is integrated using the observed SST. Figure 3 shows the tracks of the model tropical cyclones. Except the period from April to July, the tracks of the model tropical cyclone are in reasonably agreement with the observations (Fig. 4).

3.3 Impact of ENSO on the annual number of tropical cyclones

Figure 5 shows the interannual variation of annual number of the model tropical cyclones over the entire WNP, the southeast quadrant, and the other regions, respectively, together with the SST anomalies in the Niño3 region (5ºS-5ºN, 150ºW-90ºW). Their lag composites against the SST anomalies in the Niño3 region are also shown in Fig. 6 in percentile.   The lag 0 corresponds to the model El Niño developing year.

The CGCM simulates the quasi-periodic (4-5 years) ENSO with the larger amplitude than the observations (Fig. 5). EOF analysis for SST anomalies in the tropical Pacific reveals that ENSO signal is much stronger than the observations (not shown), implying that the results of the CGCM used in the present study are suitable for analyzing the relation between activities of tropical cyclones and ENSO.

As same in the observations (e.g. Lander, 1993), the annual number of the model tropical cyclones formed in the southeast quadrant of the WNP increases in the developing years of the El Niño, while there are less tropical cyclones in the La Niña years. Figure 7 shows the genesis locations of the model tropical cyclones in the El Niño years and the La Niña years. It is found that the genesis locations of the model tropical cyclones move southeastward in the El Niño years, while they move northwestward

in the La Niña years, which is consistent with the observational evidence (e.g. Wang and Chan, 2002). However, there is no significant change in the annual total number of the model tropical cyclones, because the changes in the southeast counteracts to those in the northwest (Fig. 6).
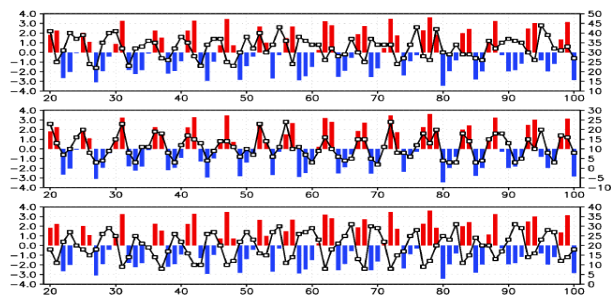

Figure 5: The annual number of the model tropical cyclones over the WNP, the southeast quadrant, and the other regions, respectively. Color bars indicate SST anomalies over the Niño3 region in July-September. Red (blue) bar corresponds to positive (negative) SST anomaly.
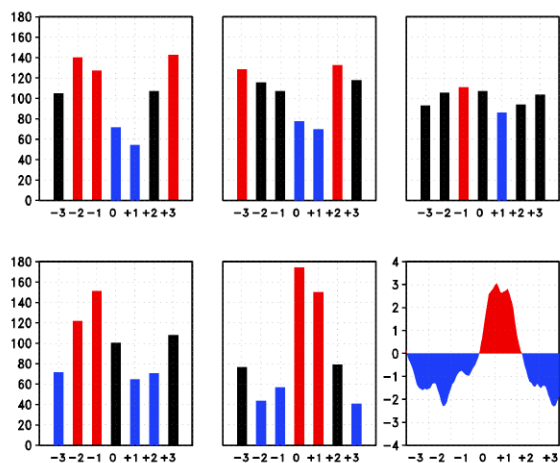

Figure 6: The lag composites of the annual number of the model tropical cyclones in the northwestern (a), southwestern (b), northeastern (c), southeast quadrant of the WNP (d), and the entire WNP, respectively, to the SST anomalies in the Niño3 region. Unit is percentile relative to climatological mean. The lag composite of SST anomalies in the Niño3 region are presented in (e). Red or blue bar indicates the statistically significant change.
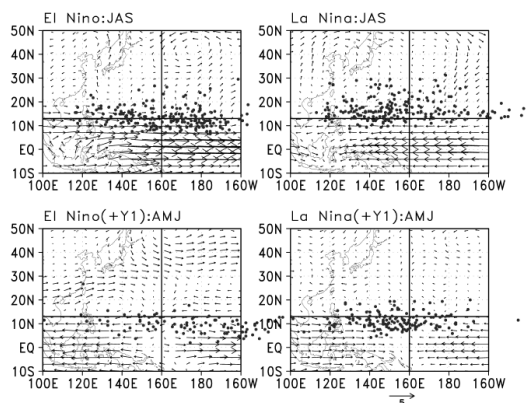

Figure 7: Genesis locations of the model tropical cyclones in July-September (JAS) of El Niño years (upper left), JAS of La Niña years (upper right), April-June (AMJ) of the following years of El Niño (lower left), and AMJ of the following years of La Niña (lower right), respectively. Surface wind anomalies are also shown.

On the other, the annual total number of the model tropical cyclones tends to decrease in the following years of the El Niño, while they increase in the following years of the La Niña. The decrease (increase) of the annual number of the model tropical cyclones is related to the development of anticyclonic (cyclonic) circulation in the Philippine Sea in response to the warm (cold) SST anomalies in the central and eastern equatorial Pacific (Fig. 7). These relationships between the annual number of the tropical cyclones and ENSO are also consistent with the observational evidence (e.g. Lander, 1993; Wang and Chan, 2002).

3.4 Impact of ENSO on the tracks

Figures 8-10 show the formation and disappearance positions of observed tropical cyclones in each season during the El Niño and La Niña years, respectively. In the present study, we define 8 El Niño years (1965, 1972, 1976, 1982,

4

1987, 1991, 1997, and 2002), and 8 La Niña years (1964, 1967, 1970, 1971, 1973, 1975, 1988, and 1999), respectively, using the SST anomalies over the Niño 3 region during summer and fall (June-November). We also note that each season used in the following is defined, considering the phase of the climatological intraseasonal oscillations (Wang and Xu, 1997), the seasonality of tropical cyclones in the WNP (Nakazawa, 1992; Kawamura et al., 1994, Ueda et al., 1995), and the seasonal change in the monsoon circulation in the WNP (Matsumoto, 1992; Ueda et al., 1995).

During late season (from 21September to 20November) of the El Niño years, the frequency of tropical cyclone formation in the southeast quadrant tends to enhance due to the anomalous low-level horizontal shear accompanied by the westerly wind anomalies in response to the warming in SST over the central and eastern equatorial Pacific, while the frequency in the southwest quadrant decreases by the anomalous descending associated with the anomalous anticyclonic circulation (Wang et al, 2000, Wang and Zhang, 2002; Wang and Chan, 2002). The reverse situations occur during late season of the La Niña years. As a result, the frequency of tropical cyclone making landfall into the Indochina Peninsula or southern China tends to reduce during late season of the El Niño years while it increases during late season of the La Niña years. On the other, tropical cyclones passing east of Japan increase in the El Niño years, while they decrease in the La Niña years. The same features are found in the tracks of the simulated tropical cyclones (Fig. 11).

In peak season (from 21July to 20September), there is the significant south-north difference in the genesis locations of observed tropical cyclones between the El Niño years and the La Niña years (Fig. 9). During the La Niña years, the frequency of tropical cyclone formation increases in the northern quadrants, while it increases in the southern quadrants in the El Niño years (Chen et al., 1998; Wang and Chan, 2002). In spite of the difference in the genesis location, however, there are not any significant differences in the number of landfalling tropical cyclones (Wu et al., 2004). During the La Niña years, the tropical cyclones formed in the northwest quadrant contribute to increase the number of landfalling tropical cyclones, while those in the southeast quadrant are related to an increase of the number of landfalling tropical cyclones during the El Niño years. The model also shows the similar features (Fig. 12), but there is the slightly difference in the number of landfalling tropical cyclones in the Indonesian Peninsula. Actually, the similar difference is found also in the observations (Fig. 9).
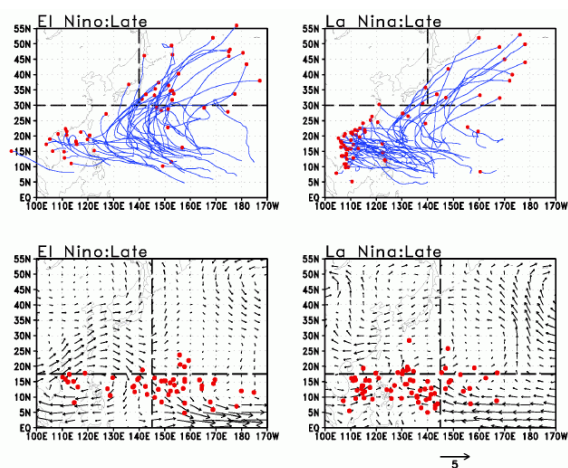

Figure 8: Locations that observed tropical cyclones are formed (lower left) and disappeared (upper left) in late season (from 21September to 20November) of the El Niño years. Right panels correspond to those in the La Niña years. Composite of low-level wind anomalies are also shown.
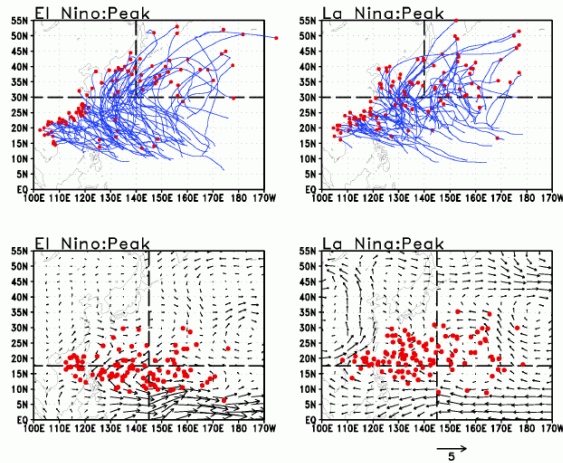
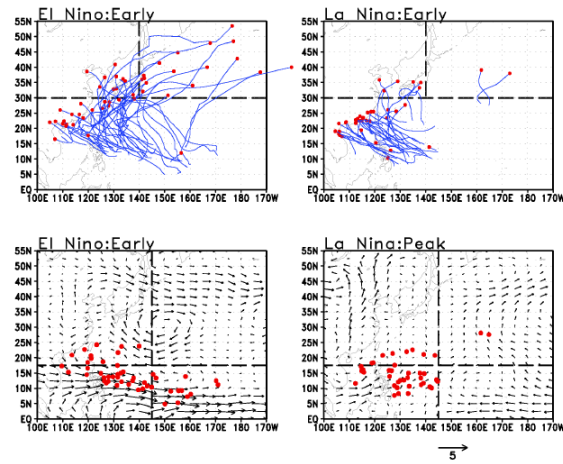Figure 9: As same in Fig. 8, but for peak season (from 21July to 20September).

Figure 10: As same in Fig. 8, but for early season (from 21May to 20July).

In early season (from 21May to 20July), the significant difference in the frequency of landfalling tropical cyclones between the El Niño and the La Niña years is found only in the observed landfalling number in the Korean Peninsula and Japan (Fig. 10). The difference is related to an increase in the frequency of tropical cyclones generated in the southeast quadrant during the El Niño years. In the model, the above difference is not clear (Fig. 13), because the model has a bias that more tropical cyclones tend to form over the central Pacific during

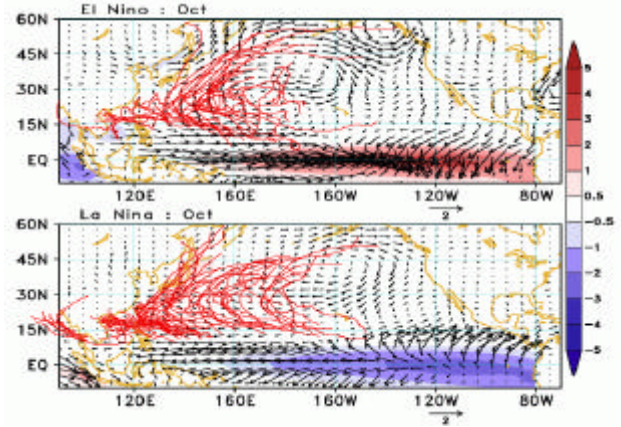the season from April to July comparing with the observations.

Figure 11: Tracks of the model tropical cyclones in October during El Niño years (upper panel) and La Niña years (lower panel), and surface wind anomalies. Shading indicates SST anomalies.
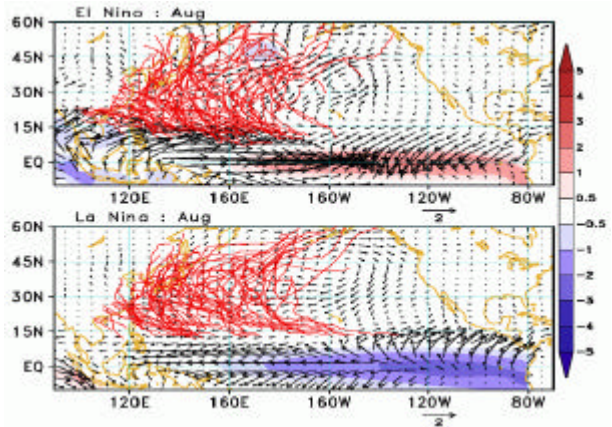

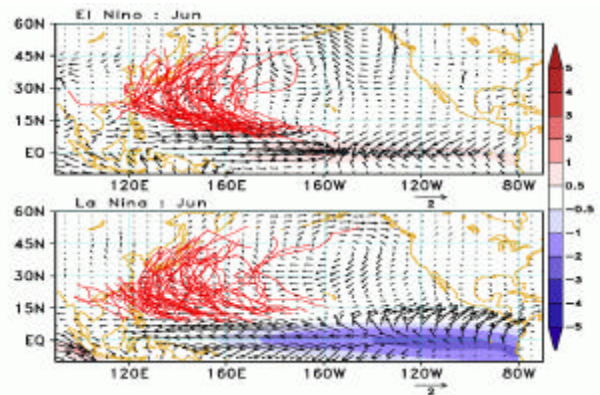Figure 12: As same in Fig. 11, but for August.

Figure 13: As same in Fig. 11, but for June.

6

4. Summary

We examined the impact of ENSO on the activities of tropical cyclones in the WNP. In the El Niño (La Niña) years, the annual frequency of the model tropical cyclones in the southeastern quadrant of the WNP increases (decreases), while it decreases (increases) in the northwestern quadrant, as in observations. In spite of the significant difference in the mean genesis locations of model tropical cyclones between El Niño and La Niña years, however, there are no significant differences in the annual frequency of model tropical cyclones in both El Niño and La Niña years. The annual frequency of model tropical cyclones, on the other hand, tends to decrease (increase) in the following El Niño (La Niña) years, relating to the development of anticyclonic (cyclonic) circulation in the Philippine Sea in response to the SST anomalies in the central and eastern equatorial Pacific.

The tracks are influenced by the change in genesis location of tropical cyclones. During boreal fall, tropical cyclones tend to recurve more northeastward during strong El Niño years, whereas most of tropical cyclones take a westward traveling course during strong La Niña years, in association with the zonal shift in the genesis location of tropical cyclones. In boreal summer, although there is the north-south shift in the genesis location of tropical cyclones between El Niño and La Niña years, there are not any significant changes in the number of landfalling tropical cyclones. The slightly difference is found only in the number of landfalling tropical cyclones in the northern part of the Indonesian Peninsula. During early summer, on the other, there is the significant difference in the observed landfalling number in the Korean Peninsula and Japan between the El Niño and the La Niña years.

The simulation of the CGCM supports the relationship between ENSO and activities of tropical cyclones described in the above, except in early summer because of the model bias.

References

Camargo, S.J., S.E. Zebiak (2002): Improving the detection and tracking of tropical cyclones in atmospheric general circulation models. Wea. Forecasting, 17, 1152-1162.

Chan, J.C.-L. (1995): Tropical cyclone activity in the western North Pacific in relation to the atmospheric quasi-biennial oscillation. Mon. Wea. Rev., 123, 2567-2571.

Chan, J.C.-L., J.E. Shi, and C.M. Lam (1998): Seasonal forecasting of tropical cyclone activity over the western North Pacific and the South China Sea. Wea. Forecasting., 13, 997-1004.

Chan, J.C.L, 2000: Tropical cyclone activity over the western North Pacific associated with El Niño and La Niña events. J. Climate, 13, 2960-2972.

Chen, T., S.-P. Weng, N. Yamazaki, and S. Kiehne, 1998: Interannual variation in the tropical cyclone formation over the western North Pacific. Mon. Wea. Rev., 126, 1080-1090.

Chia, H. H., and C.F. Ropelewski, 2002: The interannual variability in the genesis location of

tropical cyclones in the Northwestern Pacific. J. Climate, 15, 2934-2944.

Elsner, J.B., and K.B. Liu, 2003: Examining the ENSO-typhoon hypothesis. Climate Research, 25, 43-54.

Iizuka, S., K. Orito, T. Matsuura, and M. Chiba (2003): Influence of cumulus convection schemes on the ENSO-like phenomena simulated in a CGCM, J. Meteor. Soc. Japan, 81, 805-827.

Kawamura, R., T. Yasunari, and H. Ueda, 1994: Abrupt changes of seasonal evolution of large-scale convective activity and tropical cyclone over the western Pacific (in Japanese). Rep. Nat. Res. Institute for Earth Science and Disaster Prevention, 53, 1-18.

Killworth, P.D., D. Stainforth, D.J. Webb and S.M. Paterson (1991): The development of a free-surface Bryan-Cox-Semtner ocean model, J. Phys. Oceanogr., 21, 1333-1348.

Lander, M.A., 1993: Comments on "A GCM simulation of the relationship between tropical storm formation and ENSO." Mon. Wea. Rev., 121, 2137-2143.

Lander, M.A., 1994: An exploratory analysis of the relationship between tropical storm formation in the western North Pacific and ENSO. Mon. Wea. Rev., 122, 636-651.

Matsumoto, J., 1992: The seasonal changes in Asian and Australian monsoon regions. J. Meteor. Soc. Japan, 70, 257-273

Matsuura, T., M. Yumoto, and S. Iizuka (2003): A mechanism of interdecadal variability of tropical cyclone activity over the western North Pacific. Clim. Dyn., 21, 105-117.

Nakazawa, T., 1992: Seasonal phase lock of intraseasonal variation during the Asian summer monsoon. J. Meteor. Soc. Japan, 70, 597-611.

Ueda, H., T. Yasunari, and R. Kawamura, 1995: Abrupt seasonal change of large-scale convection activity over the western Pacific in northern summer. J. Meteor. Soc. Japan, 73, 795-809.

Wang, B., and X. Xu, 1997: Northern hemisphere summer monsoon singularities and climatological intraseasonal oscillation. J. Climate, 10, 1071-1085.

Wang. B., R. Wu, and X. Fu, 2000: Pacific-East Asian teleconnection: How does ENSO affect East Asian climate? J. Climate, 13, 1517-1536.

Wang. B., and Q. Zhang, 2002: Pacific-East Asian teleconnection. Part II: How the Philippine Sea anomalous anticyclone is established during El Niño development J. Climate, 13, 1517-1536.

Wang, B., and J.C.L. Chan, 2002: How strong ENSO events affect tropical storm activity over the western North Pacific. J. Climate, 15, 3252-3265.

Wu, M.C., W.L. Chang, and W.M. Leung, 2004: Impacts of El Niño Southern Oscillation events on tropical cyclone landfalling activity in the western North Pacific. J. Climate, 17, 1419-1428.

Yumoto, M., and T. Matsuura (2001): Interdecadal variability in the western North Pacific. J. Meteor. Soc. Japan, 79, 23-35.